Modeling Optical Signatures and Excited-State Reactivities of Substituted HydroxyphenylBenzOxazoles (HBO) ESIPT Dyes†: Electronic Supporting Information (ESI)

Ymène Houari[a], Azzam Charaf-Eddin[a], Adèle D. Laurent[a], Julien Massue[b], Raymond Ziessel[b], Gilles Ulrich[b] and Denis Jacquemin*[,a,c]

S1 Methods

We have used the latest revision of the Gaussian09 program[1] to perform all our computations, applying default thresholds and algorithms, except when noted below. All calculations relied on the M06-2X hybrid exchange-correlation functional,[2,3] a choice justified by numerous previous benchmarks demonstrating the accuracy of this functional for predicting both vertical and adiabatic transition energies as well as for predicting band shapes.[4–7] Here, we have applied a recently proposed strategy[5] which is to determine the geometrical and vibrational parameters with the 6-31G(d) atomic basis set, whereas the transition energies are corrected with a much more extended atomic basis set, namely 6-311+G(2d,p), so that all energies shown in the main text are corrected for basis set effects. With this approach, both vertical TD estimates and 0-0 energies (that can be compared to the experimental absorption–fluorescence crossing point)[5,8] could be obtained, which allows physically-meaningful theory–experiment comparisons.

For each molecule, both the ground and first excited states have been fully optimized using DFT/TD-DFT analytical gradients, and considering both the enol and keto forms of each HBO dye. To achieve numerically stable and accurate values, we have tightened self consistent field (10^{-10} *a.u.*) and geometry optimization (10^{-5} *a.u.*) convergence thresholds, as well as used a (99,590) pruned integration grid (so-called *ultrafine* grid). The transition states searches have been performed using quadratic synchronous transit approach (STQN) or Berny algorithms, the latter requiring an input Hessian. It is worth to point out that locating excited-state transition states was rather difficult and often required an initial relaxed scan search followed by transition-state optimization in the optimal domain. The nature of all structures, was confirmed by analytical (ground-state) or numerical (excited-state) Hessian calculations that returned 0 (minima) or 1 (transition states) imaginary vibrational modes. In addition, these calculations gave access to free energies, allowing to correct the total energy profiles (see below).

Environmental effects (here dichloromethane) have been accounted for using the well-known PCM model.[9] While geometry optimizations and Hessian have been performed with the popular linear-response (LR) PCM approach for both ground and excited-states, all excited-state energies have been corrected using the corrected LR scheme (cLR).[10,11] The cLR scheme allows to correct the cavity polarization by accounting for the change of electron density upon electronic transition. Therefore, it allows not only to compare structures having different changes of dipole moment amplitudes between the ground and excited states but also to estimate emission wavelengths (and hence Stokes shift) with more accuracy. Of course, while we applied the equilibrium PCM limit for optimization and vibrational TD-DFT calculations (slow phenomena), absorption and fluorescence wavelengths are corrected for non-equilibrium effects (fast phenomena).

In views of the two previous paragraphs, it may be useful for explain that the excited-state G energies reported in the body of the text correspond to

$$G = G^{\mathrm{LR-PCM/6-31G(d)}} + E^{\mathrm{cLR-PCM/6-311+G(2d,p)}} - E^{\mathrm{LR-PCM/6-31G(d)}}$$

Vibrationally resolved spectra have been obtained using the FCclasses program.[12–14] The reported spectra have been simulated using a convoluting Gaussian functions presenting a half width at half maximum (HWHM) that has been adjusted to allow accurate comparisons with experiments (typical value: 0.08 eV). A maximal number of 25 overtones for each mode and 20 combination bands on each pair of modes were included in the calculation. The maximum number of integrals to be computed for each class was set to 10^{12}. The Frank-Condon approximation has been employed as we consider strongly dipole-allowed ES.

For Fig. 3 in the body of the text, we have first computed the 0-0 energies following a procedure similar to the one of

[a] *CEISAM, UMR CNRS 6230, BP 92208, Université de Nantes, 2, Rue de la Houssinière, 44322 Nantes, Cedex 3, France. E-mail: Denis.Jacquemin@univ-nantes.fr.*
[b] *ICPEES-LCOSA, UMR CNRS 7575, Ecole de Chimie, Polymères, Matériaux de Strasbourg (ECPM), 25 rue Becquerel, 67087 Strasbourg, Cedex 2, France. E-mail: gulrich@unistra.fr*
[c] *Institut Universitaire de France, 103 bd St Michel, 75005 Paris Cedex 5, France.*

Ref. 5. Then, we have drawn the absorption curve from that reference points. Next, we have computed the (LR,eq) vibrationnally resolve emission (see above) and move the emission band according to the Stokes shift computed at the more accurate (cLR,neq) approach ($\Delta^{SS}_{cLR-vert}$ column in Table 2).

S2 Additional characterzations of the excited-states

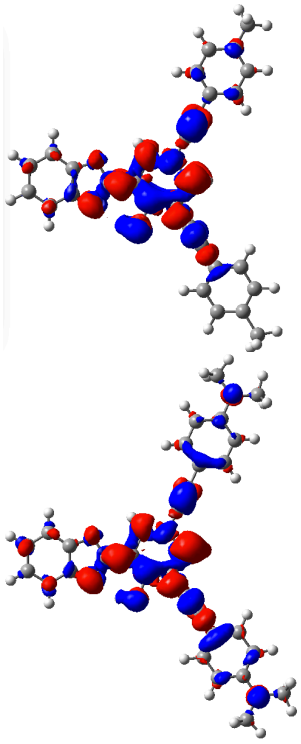

Fig. S-1 Representation of the difference between excited and ground state electronic densities for **1** (top) and **2** (bottom) considering the absorption of the enol isomers. The blue (red) regions correspond to decrease (increase) of the total density upon photon absorption. A contour threshold of 0.0008 a.u. was used for both plots.

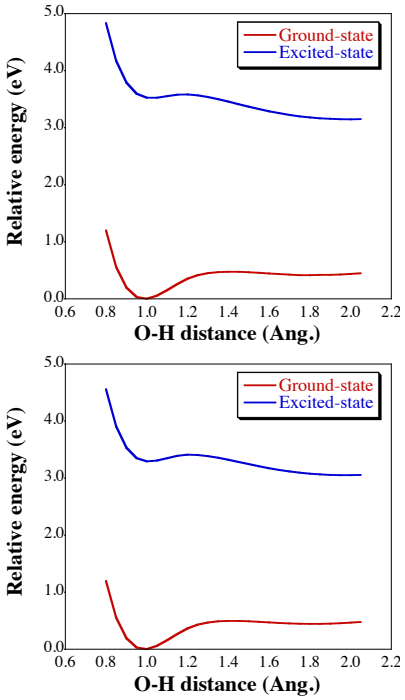

Fig. S-2 Representation of the PES obtained by relaxed S_0 and S_1 scans of the O-H distance. These scans have been performed using the LR-PCM model in its equilibrium limit, using steps of 0.05 Å between 0.80 and 2.05 Å.

S3 Data for the protonated 2

To perform our calculations on the protonated **2**, we have used HCl as in the experiment, explicitly considering the chlorine anion, so to be realistic and to avoid cavity polarization problems.[15] The obtained molecule is represented below. The geometrical and energetic data comparable to the one listed in Table 1 of the main text can be found in Table S-1.

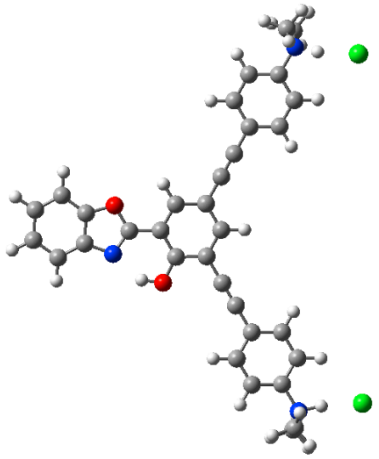

Fig. S-3 Sketch of the optimized **2**.$(HCl)_2$ molecule considering the S_0 enol form.

Table S-I Relative free energies (G in eV) and selected distances (Å) for the protonated structure.

	State	Form	G	d_{OH}	d_{NH}	$d_{O\cdots N}$
2.$(HCl)_2$	S_0	Enol	0.00	0.990	1.791	2.664
		TS	0.33	1.397	1.140	2.424
		Keto	0.37	1.834	1.029	2.596
	S_1	Enol	3.41	1.025	1.620	2.552
		TS	3.35	1.184	1.304	2.408
		Keto	3.01	2.012	1.017	2.675

S4 Additional UV/Vis Spectra

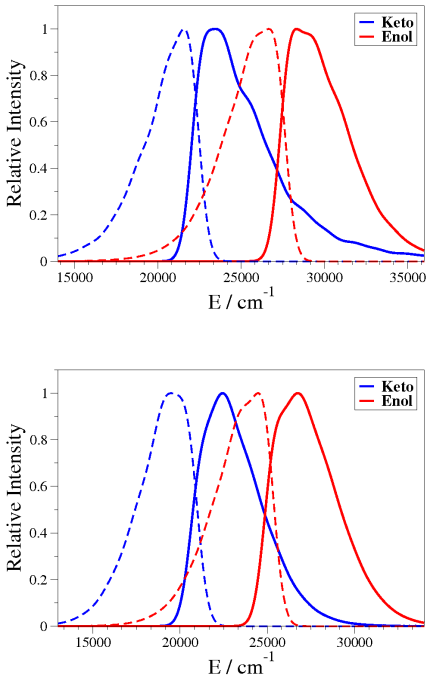

Fig. S-4 Vibrationally resolved UV/Vis spectra computed for all forms of **1** (top) and **2** (bottom) computed from the absorption-fluorescence crossing point and an uncorrected Stokes shift. The full (dashed) lines correspond to absorption (fluorescence) respectively. The red (blue) curves correspond to the enol (keto) forms.

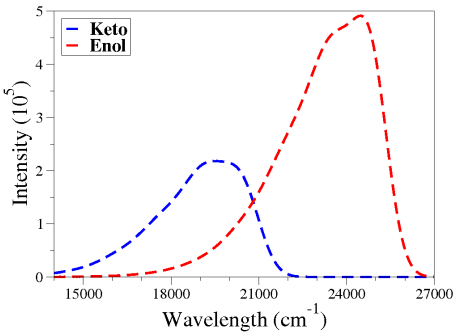

Fig. S-5 Emission of the enol and keto forms of **2** computed in terms of absolute (non-normalized) intensities.

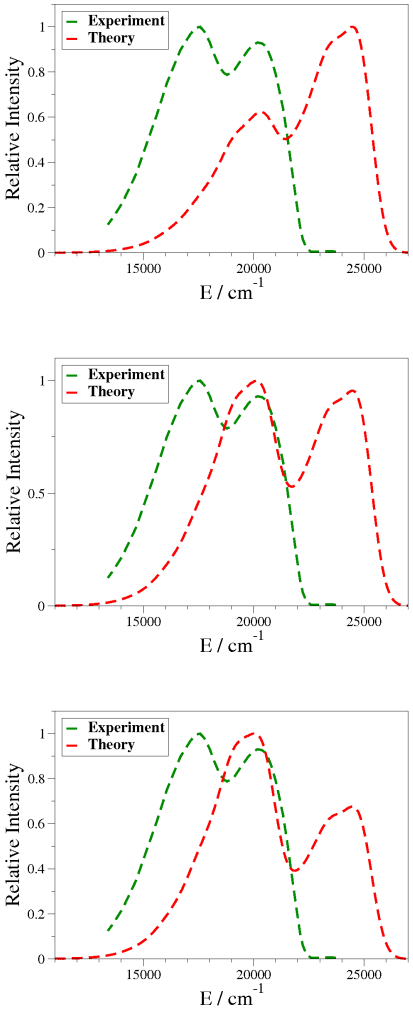

Fig. S-6 Convoluted emission of **2** for three relative enol/keto ratio: 1/1; 1/2 and 1/3 (from top to bottom).

References

1 M. J. Frisch, G. W. Trucks, H. B. Schlegel, G. E. Scuseria, M. A. Robb, J. R. Cheeseman, G. Scalmani, V. Barone, B. Mennucci, G. A. Petersson, H. Nakatsuji, M. Caricato, X. Li, H. P. Hratchian, A. F. Izmaylov, J. Bloino, G. Zheng, J. L. Sonnenberg, M. Hada, M. Ehara, K. Toyota, R. Fukuda, J. Hasegawa, M. Ishida, T. Nakajima, Y. Honda, O. Kitao, H. Nakai, T. Vreven, J. A. Montgomery, Jr., J. E. Peralta, F. Ogliaro, M. Bearpark, J. J. Heyd, E. Brothers, K. N. Kudin, V. N. Staroverov, R. Kobayashi, J. Normand, K. Raghavachari, A. Rendell, J. C. Burant, S. S. Iyengar, J. Tomasi, M. Cossi, N. Rega, J. M. Millam, M. Klene, J. E. Knox, J. B. Cross, V. Bakken, C. Adamo, J. Jaramillo, R. Gomperts, R. E. Stratmann, O. Yazyev, A. J. Austin, R. Cammi, C. Pomelli, J. W. Ochterski, R. L. Martin, K. Morokuma, V. G. Zakrzewski, G. A. Voth, P. Salvador, J. J. Dannenberg, S. Dapprich, A. D. Daniels, O. Farkas, J. B. Foresman, J. V. Ortiz, J. Cioslowski and D. J. Fox, *Gaussian 09 Revision D.01*, 2009, Gaussian Inc. Wallingford CT.

2 Y. Zhao and D. G. Truhlar, *Acc. Chem. Res.*, 2008, **41**, 157–167.

3 Y. Zhao and D. G. Truhlar, *Theor. Chem. Acc.*, 2008, **120**, 215–241.

4 M. Isegawa, R. Peverati and D. G. Truhlar, *J. Chem. Phys.*, 2012, **137**, 244104.

5 D. Jacquemin, A. Planchat, C. Adamo and B. Mennucci, *J. Chem. Theory Comput.*, 2012, **8**, 2359–2372.

6 S. S. Leang, F. Zahariev and M. S. Gordon, *J. Chem. Phys.*, 2012, **136**, 104101.

7 A. Charaf-Eddin, A. Planchat, B. Mennucci, C. Adamo and D. Jacquemin, *J. Chem. Theory Comput.*, 2013, **9**, 2749–2760.

8 L. Goerigk and S. Grimme, *J. Chem. Phys.*, 2010, **132**, 184103.

9 J. Tomasi, B. Mennucci and R. Cammi, *Chem. Rev.*, 2005, **105**, 2999–3094.

10 R. Cammi, S. Corni, B. Mennucci and J. Tomasi, *J. Chem. Phys.*, 2005, **122**, 104513.

11 M. Caricato, B. Mennucci, J. Tomasi, F. Ingrosso, R. Cammi, S. Corni and G. Scalmani, *J. Chem. Phys.*, 2006, **124**, 124520.

12 F. Santoro, R. Improta, A. Lami, J. Bloino and V. Barone, *J. Chem. Phys.*, 2007, **126**, 084509.

13 F. Santoro, R. Improta, A. Lami, J. Bloino and V. Barone, *J. Chem. Phys.*, 2007, **126**, 184102.

14 F. Santoro, V. Barone and R. Improta, *J. Comput. Chem.*, 2008, **29**, 957–964.

15 S. Chibani, B. Le Guennic, A. Charaf-Eddin, O. Maury, C. Andraud and D. Jacquemin, *J. Chem. Theory Comput.*, 2012, **8**, 3303–3313.